An Assessment of Climate Feedbacks in Coupled Ocean-Atmosphere Models

Brian J. Soden

Rosenstiel School for Marine and Atmospheric Science

University of Miami

Isaac M. Held

Geophysical Fluid Dynamics Laboratory

National Oceanic and Atmospheric Administration

Submitted to the *Journal of Climate – Letters*

Revised October 2005

Corresponding author: Dr. Brian J. Soden, Rosenstiel School for Marine and Atmospheric Science, University of Miami, 4600 Rickenbacker Cswy., Miami FL 33149.

Tel: (305) 421-4916, Fax: (305) 361-4457, email: bsoden@rsmas.miami.edu

Abstract

We compare the climate feedbacks in coupled ocean-atmosphere models using a coordinated set of 21st century climate change experiments. Water vapor is found to provide the largest positive feedback in all models and its strength is consistent with that expected from constant relative humidity changes in water vapor mixing ratio. The feedbacks from clouds and surface albedo are also found to be positive in all models, while the only stabilizing (negative) feedback comes from the temperature response. Large intermodel differences in the lapse-rate feedback are observed and shown to be associated with differing regional patterns of surface warming. Consistent with previous studies, we find the vertical changes in temperature and water vapor to be tightly coupled in all models and, importantly, demonstrate that intermodel differences in the sum of lapse-rate and water vapor feedbacks are small. In contrast, intermodel differences in cloud feedback are found to provide the largest source of uncertainty in current predictions of climate sensitivity.

Introduction

Climate models exhibit a large range of sensitivities in response to increased greenhouse gases due to differences in feedback processes which amplify or damp the initial radiative perturbation (Cubasch and Cess, 1990). Although the analysis and validation of these feedbacks are crucial tasks in climate change research, there has never been a coordinated assessment of climate feedbacks in models used for global warming projections. As a result, the relative magnitude of different feedback processes and their contributions to the range of climate sensitivities remain uncertain.

Differences in cloud feedbacks have typically been thought of as the major source of discrepancy in model sensitivity estimates, based in large part on a prominent analysis of the response of models to a uniform increase in surface temperature (Cess et al. 1990, 1996). This analysis revealed agreement among the models' clear-sky radiative flux response, but much larger discrepancies in their total-sky response, implicating clouds as key contributors to the uncertainty in climate sensitivity. However, as noted in these studies, uniform perturbations in temperature are not representative of realistic climate-change conditions and can alter the magnitude and ranking of climate feedback strengths (Senior and Mitchell 1993). The simulations were also performed using perpetual July conditions to intentionally suppress the surface albedo feedback. In addition, the cloud forcing method of feedback assessment aliases non-cloud feedbacks into the cloud forcing term; thus scatter in the cloud forcing response can partially result from differences in the total-sky components of the other feedback variables (Zhang et al. 1996, Colman 1997 and McAvaney, Colman 2003, Soden et al. 2004).

The feedback strengths from various mixed-layer GCMs forced with increasing CO_2 have been computed in prior studies. A review of these calculations by Colman (2003) revealed,

surprisingly, that intermodel differences in the reported feedbacks for clouds, water vapor, lapse-rate and surface albedo were roughly equal in magnitude (Figure 1). However, as emphasized by Colman, differences in the methodology used to compute feedbacks between various modeling groups could bias the reported feedbacks. Moreover, the survey by Colman considers only those models for which published feedback calculations are available and, as noted by Colman, many of those models were quite old. As a result, the true contribution of various feedback processes to the range in climate model sensitivity remains uncertain, particularly for the current generation of models.

Here we apply a consistent methodology to compare feedback strengths in a large group of coupled ocean-atmosphere models using a coordinated set of 21st century climate change experiments generated for the upcoming 4th Assessment of the Intergovernmental Panel on Climate Change (2).

Methodology

Feedback calculations are performed for climate change simulations from 14 different coupled ocean-atmosphere models integrated with projected increases in well-mixed greenhouse gases and aerosols as prescribed by the IPCC SRES A1B scenario (Table 1). This scenario corresponds roughly to a doubling in equivalent CO_2 between 2000 and 2100, after which time the radiative forcings are held constant. The estimated radiative forcing (the change in the global mean net radiative flux at the tropopause holding all other inputs to the radiative transfer fixed) under this scenario is 4.3 W/m^2 (IPCC TAR Table 6.14 and 6.15). The uncertainty in forcings is estimated to be ~10% for the period 1750-2000 (IPCC TAR, p. 351), which includes uncertainty in the forcing given the concentrations as well as uncertainty in the historical concentrations of

the forcing agents themselves. The uncertainty in projected forcings for 2000-2100 given the SRES A1B assumptions is presumably smaller since the concentrations of dominant forcing agents are specified. Unfortunately, the data required for directly comparing model forcings are not yet available.

We define feedbacks in terms of the change in global mean surface temperature (T_s) and the change in radiative flux at the top of the atmosphere (R). Feedbacks arise from changes in water vapor (w), clouds (C), surface albedo (α) and temperature (T). Defining a feedback parameter for each variable, we set $\Delta\overline{T}_s = \frac{\Delta\overline{R}}{\overline{\lambda}}$, where $\lambda = \lambda_T + \lambda_C + \lambda_w + \lambda_\alpha$. and the overbar indicates global averaging. The temperature feedback can be split further as $\lambda_T = \lambda_0 + \lambda_L$, where λ_0 assumes that the temperature change is uniform throughout the troposphere and λ_L (lapse rate feedback) is the modification due to non-uniformity of the temperature change.

Following Held and Soden (2000), we compute the feedbacks as products of two terms, one dependent on the radiative transfer, and another on the climatic response: $\lambda_X = \frac{\partial R}{\partial x}\frac{dx}{d\overline{T}_s}$. From the available data we are only able to compute the latter, and use a particular model for the former (GAMDT, 2004), assuming that uncertainties in the radiative algorithms, and in the distribution of radiatively active constituents in the control simulations, are small compared to the differences in model responses. Ongoing comparison of the radiative transfer component from a small subset of these models supports this assumption and indicates that we are omitting differences of the order of 10%, which would not impact our conclusions.

The model response for each variable *x* is computed by differencing the projected climate of years (2000-2010) from that of (2100-2110); $\frac{dx}{d\overline{T}_s} = \frac{x^{(2100-2110)} - x^{(2000-2010)}}{\overline{T}_s^{(2100-2110)} - \overline{T}_s^{(2000-2010)}}$. The response is

then scaled by the appropriate radiative adjoint ($K_X = \frac{\partial R}{\partial x}$) to yield the climate feedback parameter for that variable, $\lambda_X = K_X \frac{dx}{d\overline{T}_s}$, where both K_x and dx are functions of latitude, longitude, altitude and monthly-resolved season. Each λ_x is then vertically-integrated from the surface to the tropopause (defined as 100mb at the equator and increasing linearly with latitude to 300mb at the poles) and globally-averaged to yield global feedback parameters.

Thus, we perturb only the tropospheric state in the feedback computation, but we examine the response of TOA fluxes, rather than the tropopause fluxes, to these perturbations It can be shown that this is equivalent to assuming that the net dynamical heating of the stratosphere is unchanged, and that we can ignore the response of stratospheric temperatures to the change in tropospheric temperature, water, and clouds. In our experience, it is preferable to make these simplifications rather than attempt to define changes in GCM fluxes at the tropopause; the latter are sensitive to arbitrariness in the definition of the tropopause and to the movement of the tropopause as climate changes.

To compute K_x, we first calculate the control TOA radiative fluxes using 3-hourly values of temperature, water vapor, cloud properties and surface albedo from a control simulation of the GFDL GCM. For each level *k*, the temperature is increased by 1 K and the resulting change in TOA fluxes determines $\frac{\partial R}{\partial T_k}$. Similarly, $\frac{\partial R}{\partial w_k}$ is computed by perturbing the water vapor in each layer by holding relative humidity constant and increasing the temperature used to compute the saturation mixing ratio by 1 K. For $\frac{\partial R}{\partial \alpha}$, a 1% decrease in surface albedo is used to compute the TOA flux perturbation. Figure 2 displays the zonal-mean, annual-mean distribution of K_x for temperature, water vapor, and surface albedo. The reader is referred to Held and Soden (2000)

for further discussion of this method and interpretation of the spatial structure of the feedback kernels.

Using this method, we compute the climate feedbacks (λ_x) for water vapor, temperature and surface albedo. Due to nonlinearities in the calculation of K_x arising from changes in the vertical overlap of clouds, λ_c is computed as the residual difference between the effective climate sensitivity (λ_{eff}) and the sum of the other feedbacks. That is, $\lambda_c = \lambda_{eff} - (\lambda_T + \lambda_w + \lambda_\alpha)$, where $\overline{\lambda}_{eff} = \frac{\overline{G} + \Delta\overline{R}}{\Delta\overline{T}_s}$ (Murphy, 1995), $\Delta\overline{T}_s$ is the change in surface air temperature between the years (2000-2010) and (2100-2110) of the model integration. The radiative forcing for the SRES A1B scenario is estimated to be $\overline{G}$ = 4.3 W/m^2.with an uncertainty of 10% (IPCC TAR, Table 6.14). The strength of this approach is that it provides a consistent and economical method of intercomparing feedbacks among different models. Therefore, intermodel differences in climate feedbacks arise solely from differences in their climate response and not from differences in methodology. The weakness of this approach is that cloud feddback is not computed directly but only as a residual.

As verification of this strategy, we have compared the feedbacks estimated from this method with those derived using the traditional approach in which the partial radiative perturbation for each feedback variable is computed using offline radiative transfer calculations (Wetherald and Manabe 1988; Colman 2001). These results indicate that, for the GFDL GCM the water vapor, temperature and surface albedo feedbacks computed using the feedback kernels (K_x) agree with those computed using the partial radiative perturbation method to within ~5%. Computation of the feedbacks using an alternative model's K_x alters the feedback strengths by < 10%.

Because cloud feedback is computed as a residual term, it is affected by two sources of error:

1) uncertainties in the estimation of other feedbacks; and 2) uncertainties in the estimate of the effective climate sensitivity which, in turn, depends upon errors in the estimated radiative forcing. To estimate the first source of error, we have examined climate change experiments using specified SST perturbations (Soden et al. 2004) enabling the component of error in the cloud feedback residual which arises solely from the use of the kernels to be directly compared with that obtained from a partial radiative perturbation analysis of the same experiment. This comparison suggested errors of ~0.1 W/m^2/K. Since the radiative forcing calculations are not available for the IPCC model simulations, we assume a radiative forcing for the SRES A1B scenario of $\overline{G}$ = 4.3 W/m^2 with an uncertainty of +/- 10% (IPCC, TAR). For $\Delta\overline{T}_s$ ~2K, this corresponds to an uncertainty in λ_{eff} of ~0.2 W/m^2/K and likely represents the largest source of uncertainty in the cloud feedback estimate. Assuming that these two sources of error are uncorrelated, the total error is estimated to be the root of their squared sums: ~0.22 W/m^2/K or ~10%. The uncertainty estimates for all feedback variables are plotted as error bars in Figure 1.

Results

Figure 1 shows our estimates of the climate feedback parameters for lapse-rate, water vapor, cloud, and surface albedo for each of the IPCC AR4 models for which the necessary data was available. The results are also listed in Table 1. The sign convention is such that positive values indicate an amplification of the climate change (i.e., a positive feedback). The strength of λ_0 (Table 1) ranges from roughly -3.1 to -3.2 W/m^2/K. Intermodel differences in λ_0 arise from different spatial patterns of warming; models with greater high latitude warming, where the temperature is colder, have smaller values of λ_0. On average, the strongest positive feedback is due to water vapor (1.8 W/m^2/K), followed by clouds (0.68 W/m^2/K), and surface albedo (0.26

$W/m^2/K$). The troposphere warms faster than the surface in all models resulting in a negative lapse-rate feedback (-0.84 $W/m^2/K$). The intermodel variability in these feedbacks is addressed below.

As compared to the survey by Colman, the range of feedback strengths computed here is smaller for all feedbacks except clouds. The smaller range noted here could indicate an actual reduction in feedback differences in the current generation of models. However, it is more likely to result in large part from the lack of a consistent methodology in previous studies. In particular, the lapse-rate feedbacks are significantly larger here than in previous results, which may reflect the inappropriate inclusion of stratospheric temperature responses in the calculations performed by some modeling groups (Colman 2003, Held and Soden 2000). The surface albedo feedbacks are somewhat smaller in magnitude compared to those reported by Colman. Both the magnitude and intermodel range of surface albedo feedback are consistent to within ~10% of those estimated by Winton (2005) for the IPCC AR4 models.

Despite the large intermodel differences in water vapor feedback, all models exhibit a nearly constant RH behavior for their moisture response. To demonstrate this, we have recomputed the water vapor feedback for each model using the simulated temperature response and an assumption of fixed relative humidity (r) to compute the change in water vapor mixing ratio In all models, the actual strength of water vapor feedback agrees to within 5% of that computed under the assumption of fixed relative humidity (open circles in Figure 1). Interestingly, the true feedback is consistently weaker than the constant relative humidity value, implying a small but robust reduction in relative humidity in all models on average, as weighted by the water vapor kernel.

Because all models exhibit a nearly constant RH behavior, most of the scatter in λ_w stems

from differences in the lapse-rate response between models rather than from diverging responses of the relative humidity field. That is, models with a larger tropospheric warming (more negative lapse-rate feedback) also have a larger tropospheric moistening (more positive water vapor feedback) and, as noted by Colman, intermodel differences in water vapor and lapse rate feedbacks largely offset each other (Figure 3a). Because temperature and water vapor changes are so tightly coupled in models, it is logical to consider the combined lapse-rate plus water vapor feedback, rather than each term individually (Held and Soden 2000). This combined feedback is slightly larger in magnitude (0.95) than the cloud feedback and the intermodel range is significantly diminished. (Figure 1).

The range in lapse-rate feedbacks between models, in turn, stems from different meridional patterns of surface warming. Models with relatively larger warming at low latitudes have a greater reduction in lapse-rate and thus a larger (more negative) lapse rate feedback (Figure 3b). This behavior reflects the weaker coupling of the surface to the free troposphere at high latitudes compared to low latitudes where the model-simulated temperature response closely follows a moist-adiabat regardless of the convection scheme (Santer et al., 2005).

Keeping in mind the limitations of computing cloud feedbacks as a residual, and the lack of precise information on radiative forcing in the models, our results are consistent with differences in cloud feedbacks being the largest contributor to intermodel differences in climate sensitivity(Figure 1). The standard deviation in cloud feedback (0.37) is roughly 4 times larger than for the combined lapse-rate plus water vapor (0.10) or surface albedo (0.08) feedbacks. Stated differently, our direct estimates of water vapor, lapse rate, and albedo feedbacks fall far short of explaining the intermodel differences in the magnitude of global mean warming. This conclusion is consistent with early studies which suggested that cloud feedback is the largest

uncertainty in model projections of global warming (Cess et al., 1990, 1996).

One may ask whether the reduced range of water vapor and lapse-rate feedbacks noted for the IPCC AR4 models represents a convergence of model physics or simply the use of a common methodology for quantifying the feedbacks. To examine this, we have also computed these feedbacks using output from the Coupled Model Intercomparison Project II (CMIP II; see www-pcmdi.llnl.gov/cmip), in which many of the models that contributed to the Third IPCC Assesment participated. The results, listed in Table 2, show that the range of water vapor and lapse rate feedbacks in the previous generation of CMIP II models (λ_{wv}=1.5 to 2.1, λ_L =-0.42 to -1.48) is similar to that found in the IPCC AR4 models (λ_{wv} =1.5 to 2.2, λ_L =-0.41 to -1.27). The range of combined $\lambda_{wv}+\lambda_L$ feedbacks is 0.75 to 1.26 in CMIP II and 0.81 to 1.20 in IPCC AR4. This suggests that the relatively large range of lapse-rate and water vapor feedbacks found previously in the literature likely results from differences in feedback methodology between the various modeling groups.

Finally, it is worth noting that while all models have a positive cloud feedback, roughly half of the models (for which total-sky and clear-sky fluxes are available) exhibit a reduction in net radiative cloud forcing in response to the warmer climate (Figure 4b). A similar range in the distribution of cloud feedback responses was noted by Cess et al. (1990, 1996). This apparent discrepancy arises from the effects of non-cloud feedbacks on the cloud forcing term (Zhang et al. 1994; Colman 2003; Soden et al. 2004). Thus the change in cloud forcing is not a reliable measure of the sign or absolute magnitude of cloud feedback. Note however, that the change in net cloud radiative forcing is well correlated with the cloud feedback, indicating that intermodel differences in the change in cloud forcing can be used as a surrogate for intermodel differences in cloud feedback. The correlation between the cloud feedback and the independent cloud

forcing model output is also indirect evidence that the residual computation of the former is meaningful.

Summary

Progress in reducing uncertainties in model predictions of climate sensitivity requires an accurate assessment of the differences in various feedback strengths between models. However, because calculation of model feedbacks can be both time-consuming and computationally-demanding, it has been difficult to get a reliable comparison of the strength of climate feedbacks between models. Here we assessed the strength of model feedbacks using a consistent method which has been applied to an existing model archive of 21st century climate change experiments performed for the IPCC 4th Assessment.

This analysis confirms two widely-held beliefs about the behavior of climate feedbacks in models: i) that water vapor provides the largest positive feedback and that the strength of this feedback can be estimated assuming constant relative humidity in all models; and ii) that clouds provide the largest source of uncertainty in current model predictions of climate sensitivity. This work also identifies some less well recognized aspects of climate feedbacks: i) that clouds appear to provide a positive feedback in all models; and ii) that intermodel differences in lapse-rate response stem primarily from differences in the meridional distribution of surface warming, with these differences in turn responsible for much of the intermodel spread in water vapor feedback.

While the methodology developed here can not identify which cloud types are most responsible for the discrepancies in cloud feedback, recent analyses of the changes in cloud radiative forcing from the IPCC AR4 simulations (Bony and DuFresne 2005) and from the Cloud Forcing Model Intercomparison Project (Webb et al. 2005) point to low cloud cover as a primary

culprit. Our results further indicate that while the change in cloud forcing may not accurately represent the sign or magnitude of cloud feedback, it does provide a useful metric for assessing intermodel differences in cloud feedback.

References

Bony, S. and J.-L. Dufresne, 2005: Marine boundary layer clouds at the heart of cloud feedback uncertainties in climate models, *Geophys. Res. Lett.*, in press.

Cess, RD and co-authors, 1990: Intercomparison and interpretation of climate feedback processes in 19 atmospheric GCMs, *J. Geophys. Res*., **95**, 16601-16615.

Cess, RD and co-authors, 1996: Cloud feedback in atmospheric general circulation models: An update, *J. Geophys. Res*., **101**, 12791-12794.

Colman, R, 2003: A comparison of climate feedbacks in GCMs, *Clim. Dyn*. **20**, 865-873.

Colman, R and BJ McAvaney, 1997: A study of general circulation model climate feedbacks determined from perturbed SST experiments, *J. Geophys. Res*., **102**, 19383-19402.

Cubasch, U and RD Cess, Processes and modeling, in Climate Change: The IPCC Scientific Assessment, 1990, Cambridge Univ. Press, 365 pp.

The GFDL Global Atmospheric Model Development Team, 2004: The new GFDL global atmosphere and land model AM2-LM2: Evaluation with prescribed SST simulations. *J. Climate*, **17**, 4641-4673.

Held, IM and BJ Soden, 2000: Water vapor feedback and global warming, *Ann. Rev. Energy Environ*., **25**, 441-475.

Murphy, J. M., 1995: Transient response of the Hadley Centre coupled ocean-atmosphere model to increasing carbon dioxide: Part III Analysis of global-mean response using simple models, *J. Climate*, **8**, 496-514.

Santer, B.D, and co-authors, 2005: Amplification of surface temperature trends and variability in the tropical atmosphere, *Science*, submitted.

Senior, CA and JFB Mitchell, 1993: Carbon dioxide and climate: The impact of cloud parameterization, *J. Climate*, **6**, 393-418.

Senior, CA and JFB Mitchell, 2000: The time-dependence of climate sensitivity, *Geophys. Res. Lett.*, **17**, 2685-2688.

Soden, B. J., A. J. Broccoli, and R. S. Hemler, 2004: On the use of cloud forcing to estimate cloud feedback. *J. Climate*, 17, 3661-3665.

Webb, M.A. and co-authors, 2005: On uncertainty in feedback mechanisms controlling climate sensitivity in two GCM ensembles, *Clim Dyn*., submitted.

Wetherald, RT and S Manabe, 1988: Cloud feedback processes in a general circulation model, *J. Atmos. Sci.*, **45**, 1397-1415.

Winton, MW, 2005: Surface albedo feedback estimates for the AR4 climate models, *J. Climate*, submitted.

Zhang, MH, RD Cess, JJ Hack, and JT Kiehl, 1994: Diagnostic study of climate feedback processes in atmospheric GCMs, *J. Geophys. Res*., **99**, 5525-5537.

Figure Captions:

Figure 1: Comparison of the climate feedback parameters for water vapor (λ_w), lapse rate (λ_T), the combined water vapor + lapse rate, surface albedo (λ_a), and clouds (λ_c) in units of W/m^2/K. All represents the combined feedback from water vapor, lapse rate, surface albedo and clouds. Filled circles represent results from this study using the IPCC AR4 model archive. Crosses are previously published results taken from the survey of Colman (2003). Open circles for water vapor represent the water vapor feedback computed for each of the IPCC AR4 models assuming no change in relative humidity. Vertical bars depict the estimated uncertainty in the calculation of the feedbacks for each parameter (see text for details).

Figure 2. The zonal-mean, annual-mean distribution of the feedback kernels Kx for temperature (top), water vapor (middle) and surface albedo (bottom). The units of the temperature and water vapor kernels are W/m^2/K/100mb and the units of the surface albedo kernel is W/m^2/%.

Figure 3. Left: The water vapor feedback (λ_w) for each of the 14 models plotted as a function of the lapse rate feedback parameter (λ_L). **Right**: The lapse rate feedback parameter plotted as a function of the ratio of the change in tropical-mean (30N-30S) surface temperature to global-mean (90N-90S) surface temperature. Models with greater tropical warming have a larger (more negative) lapse rate feedback.

Figure 4. **Left**: The effective sensitivity (λ_{eff}) for each of the 14 models plotted as a function of the cloud feedback parameter (λ_c). **Right**: The cloud feedback parameter plotted as a function of the change in global-mean net cloud radiative forcing per degree change in global surface temperature. Only models for which both clear sky and total sky fluxes were available are shown.

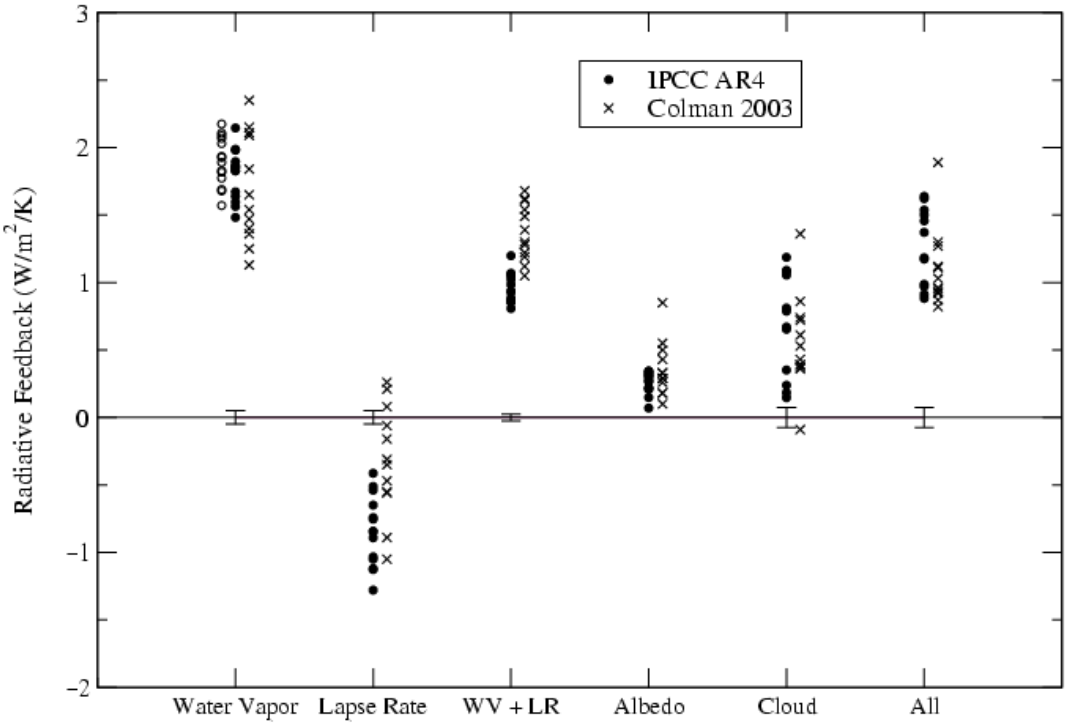

Figure 1: Comparison of the climate feedback parameters for water vapor (λ_w), lapse rate (λ_T), the combined water vapor + lapse rate, surface albedo (λ_a), and clouds (λ_c) in units of W/m^2/K. All represents the combined feedback from water vapor, lapse rate, surface albedo and clouds. Filled circles represent results from this study using the IPCC AR4 model archive. Crosses are previously published results taken from the survey of Colman (2003). Open circles for water vapor represent the water vapor feedback computed for each of the IPCC AR4 models assuming no change in relative humidity. Vertical bars depict the estimated uncertainty in the calculation of the feedbacks for each parameter (see text for details).

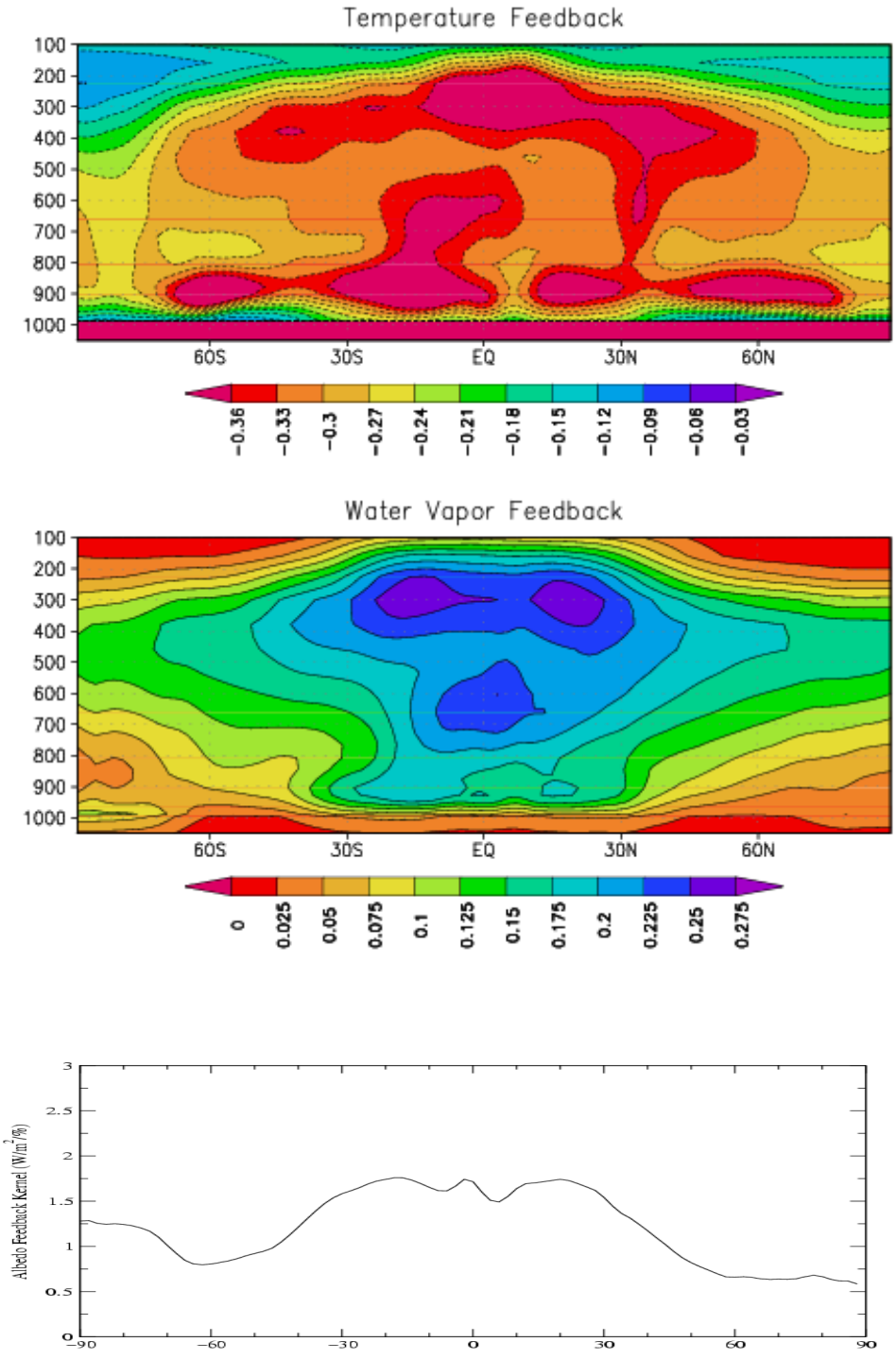

Figure 2. The zonal-mean, annual-mean distribution of the feedback kernels Kx for temperature (top), water vapor (middle) and surface albedo (bottom). The units of the temperature and water vapor kernels are $W/m^2/K/100mb$ and the units of the surface albedo kernel is $W/m^2/\%$.

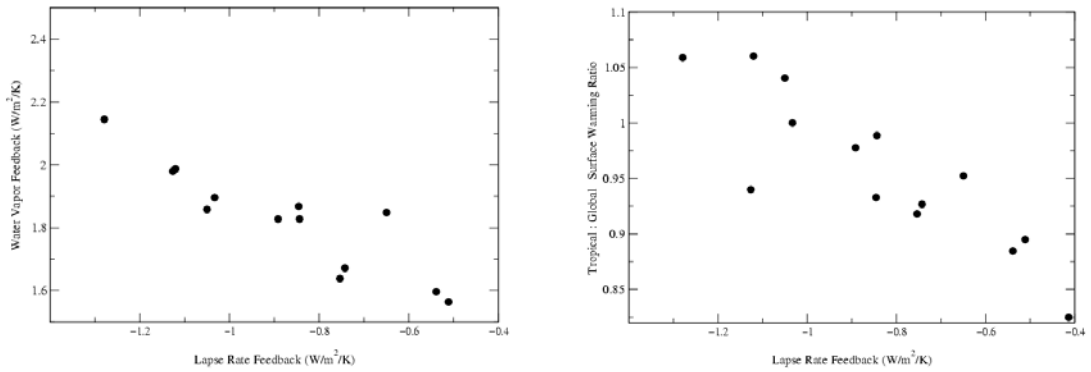

Figure 3. Left: The water vapor feedback (λ_w) for each of the 14 models plotted as a function of the lapse rate feedback parameter (λ_L). **Right**: The lapse rate feedback parameter plotted as a function of the ratio of the change in tropical-mean (30N-30S) surface temperature to global-mean (90N-90S) surface temperature. Models with greater tropical warming have a larger (more negative) lapse rate feedback.

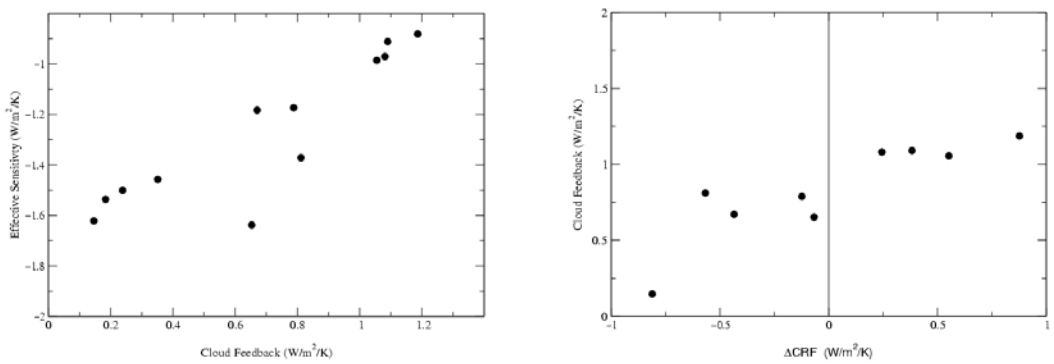

Figure 4. **Left**: The effective sensitivity (λ_{eff}) for each of the 14 models plotted as a function of the cloud feedback parameter (λ_c). **Right**: The cloud feedback parameter plotted as a function of the change in global-mean net cloud radiative forcing per degree change in global surface temperature. Only models for which both clear sky and total sky fluxes were available are shown.

	Planck	Lapse Rate	Water Vapor	Surface Albedo	Effective Sensitivity	Cloud Feedback
CNRM	-3.21	-0.89	1.83	0.31	-1.17	0.79
GFDL CM2_0	-3.20	-0.85	1.87	0.33	-1.18	0.67
GFDL CM2_1	-3.24	-1.12	1.97	0.21	-1.37	0.81
GISS AOM	-3.25	-1.27	2.14	0.27		
GISS EH	-3.26	-1.12	1.99	0.07		
GISS ER	-3.24	-1.05	1.86	0.15	-1.64	0.65
INMCM3	-3.18	-0.51	1.56	0.32	-1.46	0.35
IPSL	-3.24	-0.84	1.83	0.22	-0.98	1.06
MIROC MEDRES	-3.20	-0.75	1.64	0.31	-0.91	1.09
MRI	-3.21	-0.65	1.85	0.27	-1.50	0.24
MPI ECHAM5	-3.22	-1.03	1.90	0.29	-0.88	1.18
NCAR CCSM3	-3.17	-0.54	1.60	0.34	-1.62	0.14
NCAR PCM1	-3.13	-0.41	1.48	0.34	-1.53	0.18
UKMO HADCM3	-3.20	-0.74	1.67	0.22	-0.97	1.08

Table 1: Tabulated values of the feedback parameters shown in Figure 1. Model integrations for the GISS AOM and GISS EH models end at year 2100 and therefore estimates of the effective sensitivity and cloud feedback are not performed.

	Planck	Lapse Rate	Water Vapor
CCCM	-3.18	-0.51	1.61
CSIR	-3.24	-0.42	1.68
CSM	-3.21	-0.76	1.62
GFDL	-3.25	-0. 62	1.73
ECHO	-3.28	-1.48	2.23
ECHAM	-3.23	-1.36	2.20
HAD2	-3.25	-1.15	1.83
HAD3	-3.21	-0.75	1.51
MRI	-3.24	-1.00	2.09
PCM	-3.16	-0.66	1.62

Table 2: Tabulated values of the feedback parameters from the CMIP II model archive. The data required for computing the surface albedo feedback was not available from the archive.